Enhancement on Coulombic Efficiency of Silicon Nanowires with Interconnected Structure

Zhongsheng Wen[*], *Guanqin Wang, Song Li, Shijun Ji, Juncai Sun*

Department of Materials, Dalian Maritime University, Dalian 116026, China
[*]E-mail: zswen5@gmail.com

Interconnected silicon nanowires (Si NWs) as anode materials for lithium ion batteries are synthesized on Au-coated stainless-steel foil by the process of Chemical Vapor Deposition (CVD) based on conventional Vapor-Liquid-Gas mechanism. Relatively thick Au catalyst layer, protective gas with low thermal conductivity and rather high flow rate of source gas are tactically are tactically applied to configure the interconnected structure between Si NWs. Attractively high reversibility of the as-prepared Si NWs can be gained with an admirable Coulombic efficiency up to 91.7% even though the diameter Si NWs involved is up to 500nm. This provides an optional way to enhance the reversibility of high capacity anode materials for lithium ion batteries.

Keywords: Silicon nanowires ; high capacity; high coulombic efficiency; lithium ion batteries

1. INTRODUCTION

The rapid development of electronic devices and electric vehicles (EV) demands advanced power sources with high power density as well as long electrochemical stability [1-4]. Si has received intense attention in recent years for its high theoretical lithium insertion capacity of 4200mAh g^{-1}, prior to 372 mAh g^{-1} of commercialized graphite anode. However, the large volume expansion associated with the large quantity of lithium insertions results in structure cracking and dramatic pulverization of Si active center, and this will cause the electric disconnection of active materials, which is the main reason for the abrupt fading on the electrochemical performance of silicon anode [2, 3]. The volume changes of silicon on deep cycling can be modified effectively by the fabrication of nanostructured material. Nanostructured silicon anode materials with different dimensions have been explored for the electrodes of lithium ion batteries (LIBs) [4-24].

Researches have verified that the pulverization or cracking behavior observed in bulk or particle silicon anode do not take place on Si nanowires (Si NWs) grown directly on stainless steel despite that their Coulombic efficiency needs further improvement to meet practical applications [5,6]. Composited carbon is an admirable host for improving the Coulombic efficiency of Si NWs due to its high ionic and electronic conductivity [8-12]. However, the improvement in the efficiency comes more or less at the expense of reduced capacity due to the increased mass fraction of carbon and the correspondingly decreased fraction of silicon. Recent researches have demonstrated that interconnected structure has its superiority in improving the cycling efficiency of silicon nanowires over the conventional isolated structure. Nguyen claimed that kinked and entangled SiNWs could be prepared by the thermal gradient [13]. Interconnected SiNWs prepared from laminate catalyst of CuAl also proved the feasibility of wire net structure for the improvement of Coulombic efficiency, but the process of preparing laminate catalyst layer was relatively complicated and costly [14].

In this paper, a facile way to fabricate an interconnected SiNWs based on the traditional bottom-up mechanism was explored. The process has been mentioned in our previous work [14], by which the individual silicon NWs were linked together by Si-Au and Si particles and a high cycling efficiency was gained due to the connected structure of silicon nanowires. However, the exfoliation of Si-Au or Si particles was found in our subsequent research. It is suspected the direct interconnections between silicon nanowires should be more stable. Therefore, in this work, we prepared Si NWs directly with Au as the catalyst by similar chemical vapor deposition (CVD) process. A thick Au layer of 500 nm thickness was used as the catalyst. Ar was used as the carrier gas to create thermal gradient during depositing process. The obtained SiNWs had an unexpected morphology of an interconnected Si NW network. The highly interconnected SiNWs presented a high coulombic efficiency up to 91.7% of the first cycle, comparing with 79% efficiency correspondingly obtained with the isolated silicon nanowires [7].

2. EXPERIMENTAL

Si NWs were synthesized by the process of chemical vapor deposition (CVD), and Au is applied as the catalyst to trigger the reaction of Si self-assembling process via vapor-liquid-solid (VLS) mechanism. Au catalyst layer was pre-deposited on cleaned stainless steel substrate by electron beam. The stainless steel coated with Au catalyst was then put in a tubular furnace. Silicon nanowire was grown in a flow of pre-mixture source gas involving reactive gas (5% SiH_4 balanced by H_2) and Ar as protection gas at 500℃ for 30 min unless stated otherwise. The flow rate of reactive gas and Ar gas was kept at 250ml/min, respectively. After deposition, the substrate was taken out and mounted in 2032 coin cell case as anode without any further treatment. Li foil was used as the counter-electrode. $LiPF_6$/EC+DMC (1:1 in volume) solution was applied as the electrolyte.

The electrochemical behavior of the cells was evaluated by constant-current process at a charging-discharging current of 0.05mA between 0.02V and 1.5V. Cyclic Voltammetry was also conducted in the same voltage window with a scan rate of 0.05 mV/s. The morphology and constitutes of samples were characterized by scanning electron microscopy (Philips XL-30) and Raman

spectroscopy (Renishaw 1000). X-ray photoelectron spectroscopy (XPS) (Thermo Fishier Scientific) measurements were conducted to test the atomic ratio including in SEI (solid electrolyte interface) film. X-ray diffraction (RigakuD/MAX-3A) was also conducted to detect the phase changes.

3. RESULTS AND DISCUSSION
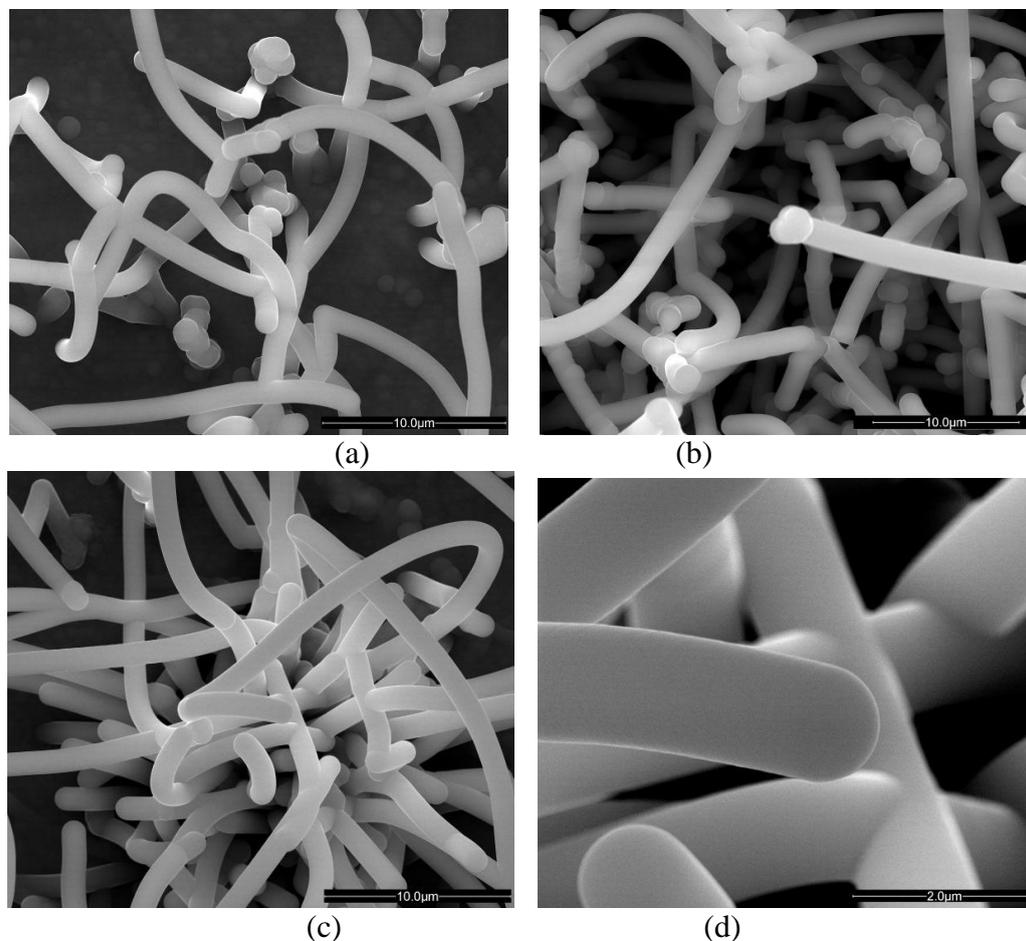
Figure 1. The SEM images of silicon nanowires deposited with different time: (a) 2min, (b) 5min, (c) and (d) 30min

The growth direction and the final morphology of silicon NWs are very sensitive to the thermal gradient. Reports mentioned that kinking in silicon nanowire occurred by control the mode of heating [10]. In our case, the silicon nanowire growth in tubular oven, where is beneficial to get long and straight nanowire because of the growth direction along with the direction of temperature increasing. In our case, Ar gas was introduced as the protective gas for its low heat conductivity, which could make the thermal field vibrating at a high flow rate and thus creating a thermal interval circumstance. High flow rate of active material could accelerate the decomposition of SiH_4. Because the eutectic point is on the tip of silicon nanowire, and the catalyst layer was thick, it is possible to get a non-uniform circumstance facilitating the precipitation of silicon phase from the eutectic. This probably is the main reason for silicon nanowires connecting together. This could be verified by the silicon

nanowire growth at different time. As shown in figure 1a-1c, the SEM images for the samples with 2min, 5min, and 30min deposition, respectively. At the beginning of deposition, the morphology of silicon nanowire is not homogeneous, which demonstrated directly the different growth rate of silicon nanowire at different spot. Connecting behavior already occurred even at the beginning of the deposition. The cross link was observed initially. When the deposition is undergoing, the merge among the silicon nanowire becomes very obviously. As shown in figure 1d, the electrode consists of smooth silicon NWs with a diameter of 500nm. These silicon NWs form an interconnected network. The interconnected structure is formed even when little quantity of silicon nanowire is deposited, which means that the individual silicon nanowire is easily connected at the beginning of depositing. Note that the diameter of silicon nanowire approaches to 500nm even at the beginning of depositing, confined by the initial diameter of Au catalysts. So the interconnecting between silicon nanowires occurring at the beginning of depositing rather than the subsequent silicon atom deposition around the silicon nanowire, different from the mechanism of silicon nanowire growth from Al-Cu catalyst [11].
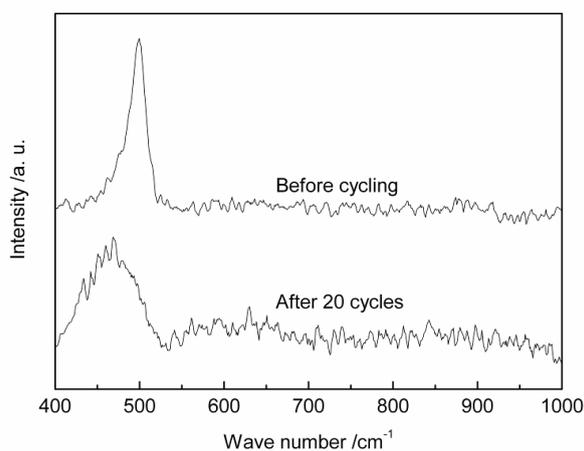
Figure 2. Raman shifts of as-prepared silicon nanowires before and after 20 cycles
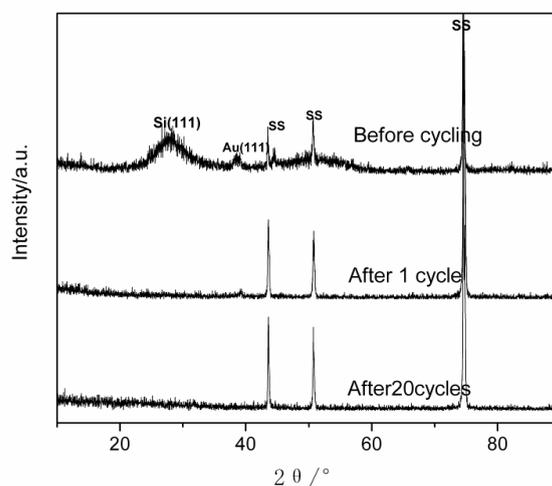
Figure 3. The XRD profiles of as-prepared silicon nanowires before and after cycling

The crystalline structure was characterized by Raman shown in figure 2. As shown in the profile before cycling in figure 2, there is a strong peak at Raman shift of 500 cm^{-1}. It is worth noting that the characteristic Raman shift of bulk crystalline silicon should appear at 521 cm^{-1} instead of 500 cm^{-1}. This means that amorphous or Wurtzite nanocrystalline structure in as-prepared Si NWs were gained in our process of CVD. Obvious shift can be observed in the profile after cycling, attributing to the structure transformation from crystal to amorphous.

The broadened silicon peak appeared at the position of 2θ=28°-30° indicated the amorphous or partially nanocrystalline structure of the as-prepared silicon nanowires (figure 3). The diffraction of stainless steel substrate was found also in the XRD patterns.

(a)   (b)
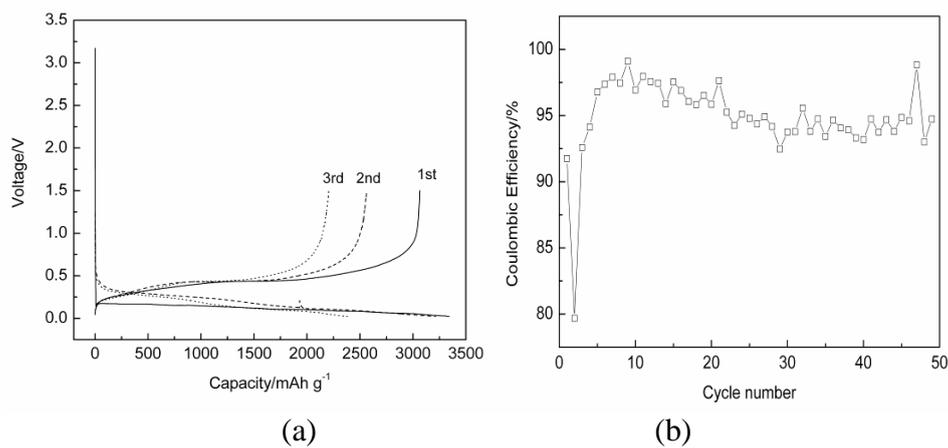
Figure 4. (a)The charge-discharge profile of silicon NWs anode for the first three cycles. (b) The Coulombic efficiency of the Si NWs anode vs cycle number

Weak Au peak can also be observed. Generally, amorphous structure is preferential for enhancing the cycling stability of silicon as the crystalline structure is definitely transferred to amorphous state along with lithium ion irreversibly inserting in the first cycle. Structure defects possess high surface energy trapping lithium ions irreversibly, so it is rational to derive that the partial nanocrystalline state involved structure of silicon nanowires is beneficial for the enhancement of coulombic efficiency. The broadened peaks of Si in figure 1 after the first cycle disappear during the subsequent cycles after the initial one. Trace of Au is also found on cycling from XRD profiles. The research on the components after cycling is still undergoing.

The Coulombic efficiency plays an important role in commercial batteries. Generally, it is very difficult to get high Coulombic efficiency especially in the first cycle for the unavoidably lithium ion trapping caused by the electrochemical decomposition of electrolyte, the structure cracking and crystal transformation [1-6]. As shown in figure 4, the intercalation behavior of lithium ions into silicon NWs for first cycle occurs below 0.1V. It is admirable that there is no obvious voltage plateau of the formation of SEI film and the voltage drops rapidly before lithium inserting, consistent with the CV behavior (figure 5). An excellent performance of high Coulombic efficiency of 91.7% with a first charge and discharge capacity of 3065mAh/g and 3341mAh/g respectively was demonstrated. The Coulombic efficiency of the subsequent cycles after the first cycle are around or more than 93%. Note

that generally it is difficult to achieve a high Coulombic efficiency for pure Si NWs or silicon nanoparticles even with a diameter under 100nm. However, in our case, the diameter of the as-prepared Si NWs is about 500 nm, so it is deduced that the amorphous involved structure as well as the interconnected structure of the Si NWs is the main reason for the enhancement of Coulombic efficiency. The starting amorphous structure avoids the irreversible lithium ion trapping due to fewer defects generated during lithium ion inserting and extracting. Moreover, the interconnected structure can make Si NWs linked even if cracking occurs.
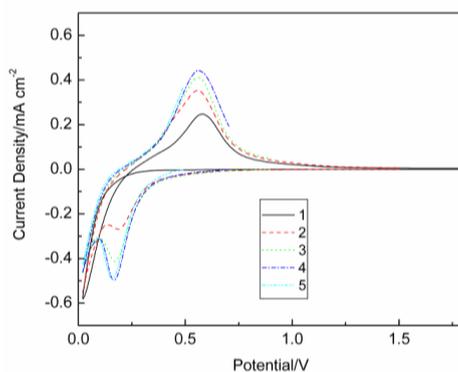
Figure 5. Cyclic voltammetry of Si NWs electrode with a scan rate of 0.05mV/s of the first 5 cycles

(a)   (b)

(c)
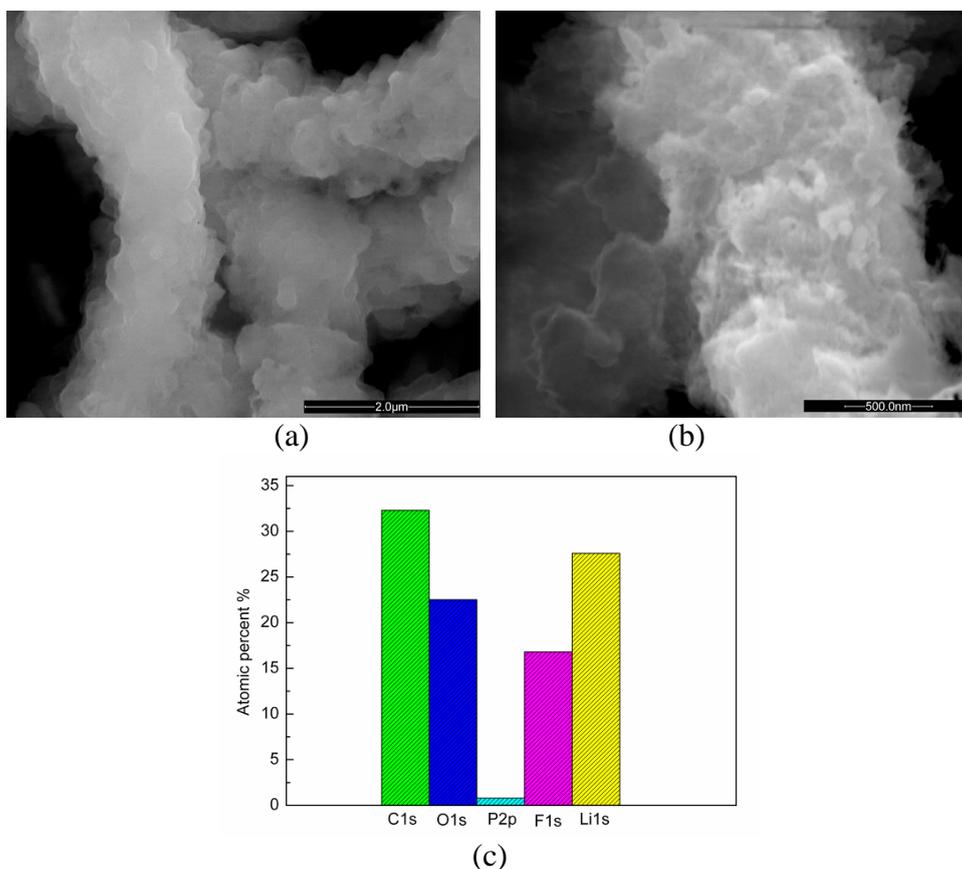
Figure 6. (a) and (b) SEM images of Si NWs electrode after cycling, (c) Atomic percent of SEI film on Si NWs electrode characterized by XPS

The measurement of cyclic voltammetry was conducted to reveal the electrochemical behavior of Si NWs during lithium insertion and extraction. One reduction peak of the first cycle at about 0v is presented in figure 5, and no any behavior related to electrolyte decomposition is found, coincident to the charge-discharge profiles. The cathodic peak for the first lithiation beginning at 0.1V is designated to the initial formation of Li-Si alloy [17, 18]. The cathodic peaks for lithiation change in the subsequent cycle with a cathodic peak appearing at 0.21V due to the Li-Si alloy with different lithium insertion [19].

The morphology and structure of silicon nanowire after cycling was characterized. The SEI film coated on the nanowires is rather dense in floccus state (figure 6a and 6b), whereas the interconnected structure of silicon NWs is remained well (figure 6a), which means the structure of silicon nanowire can resist deep charge-discharge process although large expansion happens unavoidably. This is one of the key factors to maintain long-life electrochemical performance. Conventionally, the structure transformation consumes large quantity of lithium ions, resulting in dramatic irreversible capacity on cycling, especially in the first cycle. In our case, the individual nanowires are linked to each other to form an interconnected wire net. The space among the wire net can provide extra accommodation of structure expansion during electrochemical reaction. The XPS measurement results present that the basic components involved are similar to other carbon type anode materials. Li_2CO_3, CH_3OCO_2Li and LiF exist in the surface of Si NWs. The atomic ratio of Li, C, O, F is shown in figure 6c.

4. CONCLUSION

In conclusion, the high coulombic efficiency and high capacity electrochemical performance of the Si NWs can be gained by configuring interconnected structure. Different from the conventional VLS process, relatively thick Au catalyst, protective gas with low thermal conductivity and rather high flow rate of source gas are tactically introduced to create vibrating thermal circumstances, which is beneficial to synthesis interconnected Si wire net. The first discharge capacities of as-prepared Si NWs is up to 3341mAh/g. Very attractive high Coulombic efficiency of 91.7% has been gained in the first cycle of lithium inserting into and extracting from Si NWs despite that the diameter of the yielded Si NWs is almost up to 500 nm, which demonstrates the admirable enhancement on the electrochemical reversibility by configuring interconnected structure. The Coulombic efficiency of the subsequent cycles after the first cycle are around or more than 93%. The interconnected structure of Si NWs is remained well after deep charging-discharging with similar SEI film in its surface. It demonstrates that to construct interconnected structure is a feasible way to enhance the Coulombic efficiency of Si NW electrode for lithium ion batteies.

References

1. E. Eustache , P. Tilmant , L. Morgenroth , P. Roussel , G. Patriarche , D. Troadec , N. Rolland , T. Brousse and C. Lethien, *Adv. Energy. Mater*, 4 (2014) 1301612.
2. R. A. Huggins, *J. Power Source*, 13 (1999) 81.
3. U. Kasavajjula, C. Wang, and A. J. Appleby, *J. Power Source*, 163 (2007) 1003.
4. H. Karami1, A. Mohammadi, *Int. J. Electrochem. Sci*, 10(2015)7392.
5. L. Y. Beaulieu, T. D. Hatchard, A. Bonakdarpour, M. D. Fleischauer and J. R. Dahn, *J. Electrochem. Soc*, 150 (2003) A1457.
6. C . Liu, F .Li, L .P . Ma, and H . M . Cheng, *Adv. Mater*, 22 (2010) E1.
7. C. K. Chan, H. L. Peng, G. Liu, K. McIlwrath, X. F. Zhang, R. A. Huggins and Y. Cui, *Nat. Nanotechnol*, 3 (2008) 31.
8. Q . Si, K. Hanai, N. Imanishi, M. Kubo, A. Hirano, Y. Takeda and O. Yamamoto, *J. Power Source*, 189 (2009) 761.
9. H. Kim and J. Cho, *Nano Letter*, 8 (2008) 3688.
10. H. Kim, B. Han, J. Choo and J. Cho, *Angew. Chem. Int. Ed*, 47 (2008) 10151.
11. N. Dimov, S. Kugino and M. Yoshio, *Electrochim. Acta*, 48 (2003) 1579.
12. H. -Y. Tsao and Y. -J. Lin, *Appl. Phys. Lett*, 104 (2014) 053501.
13. H. T. Nguyen, F. Yao, M. R. Zamfir, C. Biswas, K. P. So, Y. H. Lee, S. M. Kim, S. N. Cha, J. M. Kim and D. Pribat, *Adv. Energy Mater,* 1 (2011) 1154.
14. Z. Wen, J. Stark, R. Saha, J. Parker and P. A. Kohl, *J. Phys. Chem. C*, 117 (2013) 8604.
15. Z. Wen, M. Cheng, J. Sun and L. Wang, *Electrochim. Acta*, 56 (2010) 372.
16. R. Ruffo, S. S. Hong, C . K. Chan, Robert A. Huggins and Y. Cui, *J. Phys. Chem. C, 113(*2009) 11390.
17. D. Aurbach, A. Nimberger, B. Markosky, E. Levi, E. Sominski and A. Gedanken, *Chem. Mater*, 14 (2002) 4155.
18. H. Li, X. Huang, L. Chen, G. Zhou, Z. Zhang, D. Yu, Y. J. Mo and N. Pei, *Solid State Ionics,* 135 (2000) 181.
19. E. Pollak, G. Salitra, V. Baranchugov and D. Aurbach, *J. Phys. Chem. C*, 111 (2007) 11437.
20. F. Kong, R. Kostecki and G. Nadeau, *J. Power Source*, 97-98 (2001) 58.
21. H. Kim, J. Cho, *Nano Lett*, 8 (2008) 368.
22. M. N. Obrovac, L. J. Krause, *J. Electrochem. Soc*, 154 (2007) A103.
23. A. Magasinski, P. Dixon, B. Hertzberg, A. Kvit, J. Ayala, G. Yushin,. *Nat. Mater,* 9 (2010) 353.
24. E. Peled, F. Patolsky, D. Golodnitsky, K. Freedman, G. Davidi, and D. Schneier, *Nano Lett*, 15 (2015) 3907.